18th International Conference on Protection & Automation in Power System
Shahrood University of Technology
January 9, 2024 - January 10, 2024

A Comparion of the Impact of Current Priority Modes of Inverter-Based Resources on the Performance of Grid Protective Relays

Peyman Jafarian
Transmission Grid Protection Office
Iran Grid Management Company (IGMC)
Tehran, Iran
jafarian@igmc.ir

Farrokh Aminifar
School of Electrical and Computer Engineering
University of Tehran
Tehran, Iran
frkh.aminifar@gmail.com

***Abstract*— The dynamic response of inverter-based resources (IBRs) during fault-ride-though condition is driven by its control system, and it can be greatly different from that of a synchronous generator. To standardize the fault response of IBRs, the recently published IEEE Std. 2800-2022 has defined two different current control modes during abnormal voltage conditions, i.e. reactive current priority mode and active current priority mode. This paper compares these control modes based on their impacts on the grid protective relays. To do so, the reference currents generator of IBR is designed so as to utilize the maximum current capability of the IBR while complying with the requirements of the mentioned standard. Followed by modeling an IBR with its complete closed-loop control system in the PSCAD/EMTDC program, extensive simulation studies are conducted on a test power system. The obtained results indicate that the reactive current priority mode is superior for the correct operation of grid protective relays. Whereas, the active current priority mode may lead to malfunction of conventional protective relays.**

Keywords- current priority mode; grid code; inverter-based resources; grid protective relays

I. Introduction

The ever proliferating integration of renewable resources to transmission systems (TSs) has posed new challenges to power system operators. These challenges, in some respects, are driven by dynamic response of inverter-based resources (IBRs) during short-circuit faults [1]. In a full-converter interfaced IBR, the inverter has been mainly designated to inject the available active power into the grid and commonly sized only per maximum active power quantity. During short-circuit faults occurring on the grid, however, it has been designed to disconnect or continue to inject limited symmetrical currents depending on the extent of voltage drop observed at the IBR interconnection point [2]. This behavior, which is referred to as fault-ride-through (FRT) characteristic, can result in malfunctioning of some of protective relays designed based on the fault response of synchronous generators [3]-[6]. To elaborate, current-based relays including distance, differential, and overcurrent relays require a minimum current to pick up, below which the relay is not able to detect the faulty condition. Furthermore, lack of negative-sequence current contribution during unsymmetrical faults can affect some elements of protective relays which are based on the negative-sequence current information, including the directional, fault type classification, voltage transformer supervision, and distance elements [7]-[12].

From the power system perspective, lack of IBR contribution to voltage support renders the voltage depression during short-circuit faults to spread over a larger area of the grid which can turn into a concerning situation in the wake of IBRs growth. As a countermeasure, new grid codes have mandated the IBRs to be in service during the short-circuit faults and to support the grid by injecting reactive currents temporarily [13]-[14]. According to the recently published IEEE Std. 2800-2022, the IBR unit, by default, shall operate in reactive current priority mode during high and low-voltage ride-through conditions. But, if requested by the transmission system owner and mutually agreed with the IBR owner, the IBR unit may operate in active current priority mode for both high and low-voltage ride-through conditions to support the system frequency [14].

This paper studies the performance of grid protective relays under the current control modes of operation defined in the IEEE Std. 2800-2022. To do so, the reference currents generator of IBR is designed in accordance with the requirements of the mentioned standard so that the output current of the inverter during fault-ride-though operation increases up to its maximum allowable current. The IBR plant including a space-vector-modulation-based inverter and its closed-loop control system is modeled in the PSCAD/EMTDC program. Extensive simulation studies are conducted to evaluate the performance of grid protective relays under various operating conditions of the IBR, and some of the obtained results are presented.

II. High/Low Voltage-Ride-Through Requirements

Fig. 1 depicts the voltage-ride-through requirements specified by the IEEE Std. 2800-2022 for IBR plants with auxiliary equipment limitations. Most utilities have similar requirements, with some deviations [14]. The voltage value in this figure denotes the lowest value of applicable voltages at the grid connection point. For effectively grounded transmission systems, the applicable voltages shall be the phase-to-phase and phase-to-ground voltages. For remainder of systems with weak or no grounding mechanisms, the applicable voltages shall be just the phase-to-phase voltages. The dynamic currents should be injected into the grid at least for a period of time determined in the low/over voltage-ride-through requirements of the grid code. Then after, if all of the applicable voltages do not return to the normal operating range, the IBR is allowed to disconnect from the grid.

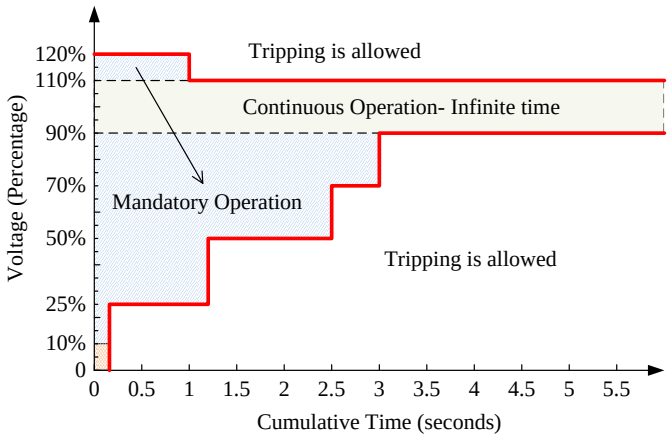

Figure 1. Typical voltage-ride-through requirements for IBR plants

During the voltage-ride-through interval, the IBR unit shall have capability to select operation in either active current priority mode or reactive current priority mode. In active current mode, the IBR current is in-phase with the voltage of IBR grid connection point and in reactive current mode, they are quadrature. The reactive current mode is desirable to support the grid voltage and protective devices. However, active current mode is desired as it can support power system frequency during faults. The IBR unit operates in reactive current priority mode during high and low-voltage ride-through events; unless mutually agreed between transmission system and IBR owners to operate IBR in active current priority mode for both high and low-voltage ride-through events [14].

A. Reactive Current Priority Mode

When operating in reactive current priority mode, priority shall be given to the reactive current injection during voltage-ride-through operation, with any residual capacity being allocated to the active current. Hence, the active power injection is significantly cut off or zeroed if necessary. For balanced faults, an IBR unit shall inject positive-sequence reactive current in respect to IBR terminal voltage. The difference between reactive current injection during a fault and a pre-fault reactive current output is an incremental positive-sequence reactive current (ΔIR-1) that shall not be negative.

For unbalanced faults, in addition to increased positive-sequence reactive current, the IBR unit shall inject negative-sequence current dependent on the negative-sequence voltage at the point of connection that leads the negative-sequence voltage by an angle between 90~100 degrees. Assuming the pre-fault negative-sequence current is zero or negligible, the negative-sequence reactive current injection during a fault is an incremental current (ΔIR-2).

If the IBR total current exceeds its limit, either or both ΔIR-1 and ΔIR-2 needs to be cut down with a preference of equal reduction in both currents. Additionally, the incremental positive-sequence reactive current injection shall not be less than the incremental negative-sequence reactive current [14].

B. Active Current Priority Mode

Active current priority mode provides benefits for power systems with low inertia. When the IBR unit is specified to operate in active current priority mode, injection of the available active current is prioritized up to the IBR maximum current rating, and the remaining capacity is used to inject reactive current. Accordingly, the IBR ability to inject reactive current is most likely limited in this mode.

III. Proposed Reference Currents Generator

Fig. 2 depicts a full-converter interfaced IBR including its closed-loop control system. According to the IEEE Std. 2800-2022, the default reference point of applicability for the current injection during voltage-ride-through mode should be the point of connection of the IBR unit (POC). The proposed reference currents generator consists of two blocks: the initial dynamic reactive currents calculator and the final reference generator.

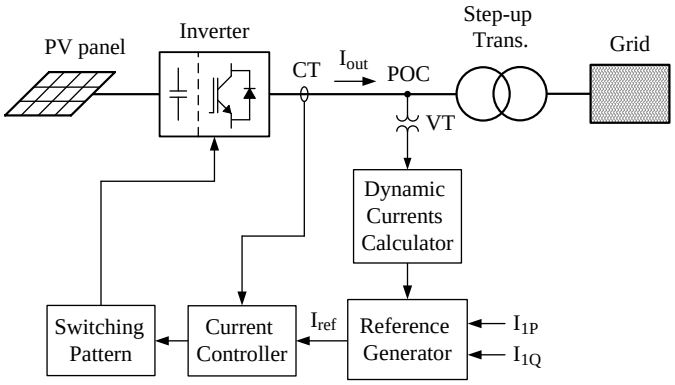

Figure 2. Block diagram of closed-loop control system of a full-converter interfaced IBR

The first block calculates the initial values of the dynamic positive- and negative-sequence reactive currents regardless of the current control mode. These values are obtained from

$$\Delta I_1 = k_1 \cdot \Delta|V_1| * 1^{\angle\theta_1+90^\circ} \quad (1)$$

$$\Delta I_2 = k_2 \cdot \Delta|V_2| * 1^{\angle\theta_2+90^\circ} \quad (2)$$

where θ_1 and θ_2 are the phase angle of positive- and negative-sequence voltages at the POC, respectively, and k_1 and k_2 are two adjustable coefficients. Besides, $\Delta|V_1|$ and $\Delta|V_2|$ are the changes in the magnitude of positive- and negative-sequence voltages defined as follows:

$$\Delta|V_1| = \frac{|V_1| - |V_{1\_1min}|}{V_n} \quad (3)$$

$$\Delta|V_2| = \frac{|V_2| - |V_{2\_1min}|}{V_n} \quad (4)$$

where V_n denotes the nominal voltage at the POC. It is worth noting that an IBR with gradient k_1 from 2 to 6 will emulate a synchronous generator (SG) with a subtransient reactance in the typical range from 0.12 to 0.4 pu [1]. Similarly, gradient k_2 emulates the negative-sequence reactance of the SG. Fig. 3 depicts the characteristics of the above described dynamic reactive currents capability. The dead-band shown in the figure provides an insensitivity range configurable in the range of 0% to 15%.

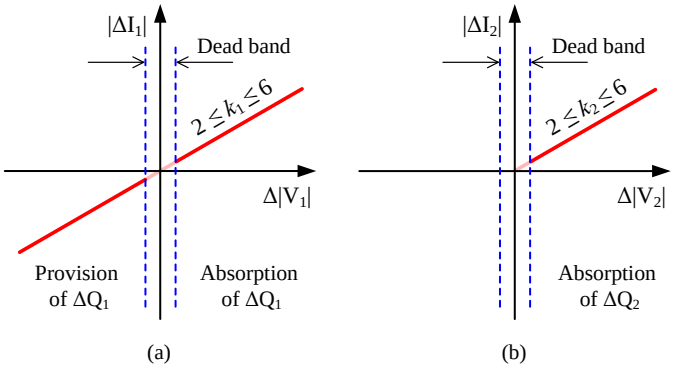

Figure 3. Dynamic reactive current support by IBR, (a) positive-sequence current, (b) negative-sequence current

Fig. 4 illustrates the proposed scheme for calculation of the dynamic reactive currents. The three-phase voltages at the POC are measured continuously, and their symmetrical components are calculated using Fortescue transform. To have a robust estimation for the magnitude of pre-disturbance voltage, the mean value of voltage within one minute is calculated continuously using a moving data window algorithm. When the disturbance detector (DD) detects a high/low voltage-ride-through condition, the pre-disturbance voltage is hold until the voltage returns to its normal range. The DD is a simple algorithm that operates based on the deviation of the positive- and negative-sequence voltages beyond the dead-bands specified in Fig. 3.

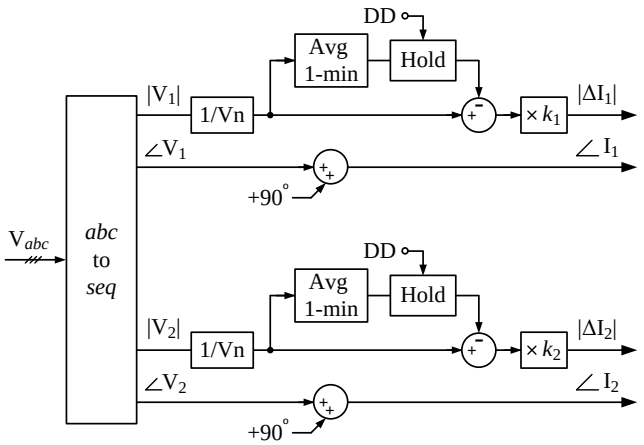

Figure 4. Proposed scheme for calculation of the dynamic reactive currents

Under normal conditions, the reference of positive-sequence currents is calculated in such a way that the available active power is injected to the grid with a power factor according to the reactive power capability required by the grid code requirements. When DD triggers the voltage-ride-though operation, the dynamic currents come into effect and the reference currents will be calculated depending on the current priority mode.

A. Proposed Refrence Generator for Reactive Current Priority Mode

Fig. 5 illustrates the flowchart of the proposed reference currents generator to comply with the voltage-ride-through requirements of the IEEE Std. 2800-2022. This algorithm considers the inverter limitation in all three phases simultaneously, while utilizing the maximum current capability of the IBR. To do so, the reference currents are calculated so that the phase current with largest amplitude is limited to the maximum allowable current.

As mentioned previously, the incremental positive-sequence reactive current cannot be negative. Therefore, if the magnitude of dynamic positive-sequence reactive current calculated in (1) is smaller than the pre-disturbance reactive current (I_{1Q}), it should be increased to I_{1Q}. The pre-disturbance reactive current is, indeed, its mean value within one minute that is held when DD triggers the over/under voltage-ride-though operation.

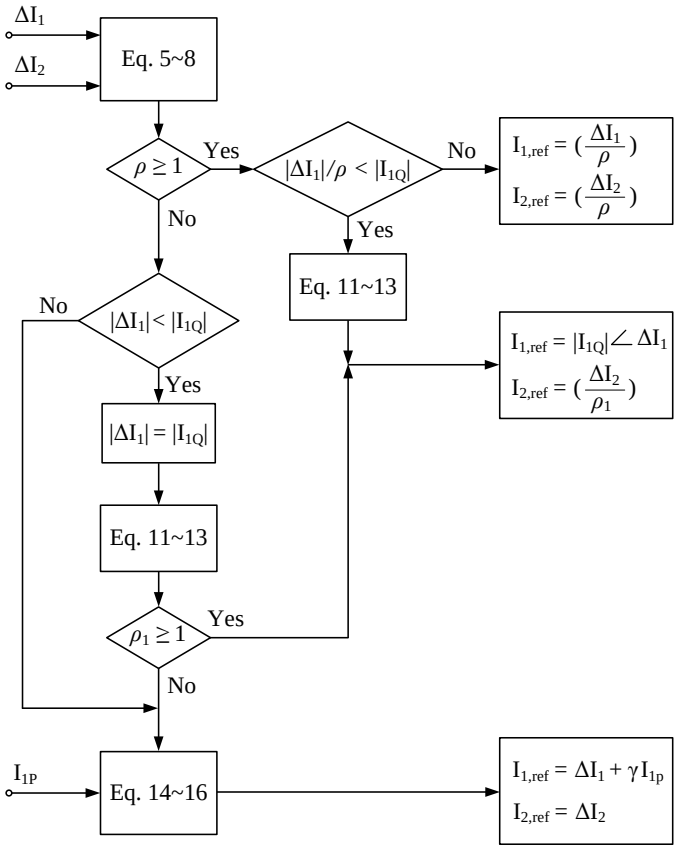

Figure 5. Proposed reference currents generator for reactive current priority mode

Depending on the amount of change in the sequence voltages and the adjusted gains for the dynamic characteristics, the magnitude of the reference currents may exceed the maximum allowable current of the inverter (I_{max}). The dynamic currents in the phase domain are given by

$$\Delta I_A = \Delta I_1 + \Delta I_2 \quad (5)$$
$$\Delta I_B = a^2 \Delta I_1 + a \Delta I_2 \quad (6)$$
$$\Delta I_C = a \Delta I_1 + a^2 \Delta I_2 \quad (7)$$

where a is the phase shift operator, $1\angle 120°$. To avoid violating the current limit in all three phases, a maximum operator is utilized to set the moderator factor ρ:

$$\rho = max\left(\frac{|\Delta I_A|}{I_{max}} \ , \ \frac{|\Delta I_B|}{I_{max}} \ , \ \frac{|\Delta I_C|}{I_{max}}\right) \quad (8)$$

When ρ exceeds 1, it is necessary to reduce the reference of dynamic currents sufficiently. However, the dynamic positive-sequence reactive current should not be smaller than the pre-disturbance reactive current. Thus, if the dynamic positive-sequence reactive current divided by ρ is greater than I_{1Q}, both dynamic positive- and negative-sequence currents are reduced by the same amount as follows:

$$I_{1,ref} = \Delta I_1 / \rho \quad (9)$$
$$I_{2,ref} = \Delta I_2 / \rho \quad (10)$$

Otherwise, the reference of positive-sequence reactive current is considered to be equal to I_{1Q}, and only the dynamic negative-sequence reactive current is reduced. In this condition, the currents magnitudes in the phase domain are given by

$$|\Delta I_A| = |I_{1Q} + \Delta I_2 / \rho_1| \quad (11)$$
$$|\Delta I_B| = |a^2 I_{1Q} + a \Delta I_2 / \rho_1| \quad (12)$$
$$|\Delta I_C| = |a I_{1Q} + a^2 \Delta I_2 / \rho_1| \quad (13)$$

Equating (11)-(13) with I_{max} will give three answers for ρ_1, of which the maximum value is selected to limit the current with largest magnitude to I_{max}.

When the moderator factor ρ calculated in (8) is smaller than 1, a free capacity may be available to inject all or a portion of the IBR available active power into the grid, as well as the dynamic reactive currents. However, it should be first verified that the dynamic positive-sequence reactive current is greater than the pre-disturbance reactive current. If not, the reference of positive-sequence reactive current is considered to be equal to I_{1Q}. Then, the moderator factor of the negative-sequence current (ρ_1) is calculated using (11)-(13). If the obtained value for ρ_1 is greater than 1, not only does zero capacity exist to inject active current, but even should the dynamic negative sequence current be reduced accordingly.

Otherwise, there is no need to reduce the dynamic negative-sequence reactive current, and meanwhile a capacity is free to inject a portion of the available active current. In this condition, the currents magnitudes are given by

$$|\Delta I_A| = |\gamma I_{1P} + \Delta I_1 + \Delta I_2| \quad (14)$$
$$|\Delta I_B| = |a^2(\gamma I_{1P} + \Delta I_1) + a \Delta I_2| \quad (15)$$
$$|\Delta I_C| = |a(\gamma I_{1P} + \Delta I_1) + a^2 \Delta I_2| \quad (16)$$

Equating (14)-(16) with I_{max} gives three positive answers for γ, of which the minimum value is selected to ensure no violation occurs in any of three phases.

B. Proposed Refrence Generator for Active Current Priority Mode

Fig. 6 illustrates the flowchart of the proposed reference currents generator for the active current priority mode. In this mode of operation, the reference of positive-sequence active current is calculated so as to inject the available active power into the grid.

$$I_{1P} = \frac{P_{available}}{3\,|V_1|} * 1^{\angle \theta_1} \quad (17)$$

It is worth noting that due to the voltage drop caused by the fault occurrence, it is possible that the magnitude of the active current calculated in (17) exceeds the maximum allowable current of the inverter. If so, the reference current should be limited to I_{max}. Otherwise, the residual capacity is used to inject all or a portion of the dynamic positive- and negative-sequence reactive currents calculated previously by the proposed scheme in Fig. 4. In this condition, the currents magnitudes are given by

$$|I_{A,ref}| = |I_{1P} + \Delta I_1 / \rho_2 + \Delta I_2 / \rho_2| \quad (18)$$

$$\left|I_{B,ref}\right| = \left|a^2(I_{1P} + \Delta I_1/\rho_2) + a\Delta I_2/\rho_2\right| \quad (19)$$

$$\left|I_{C,ref}\right| = \left|a(I_{1P} + \Delta I_1/\rho_2) + a^2\Delta I_2/\rho_2\right| \quad (20)$$

Equating (18)-(20) with I_{max} will give three answers for ρ_2, of which the maximum value is selected to limit the current with largest magnitude to I_{max}.

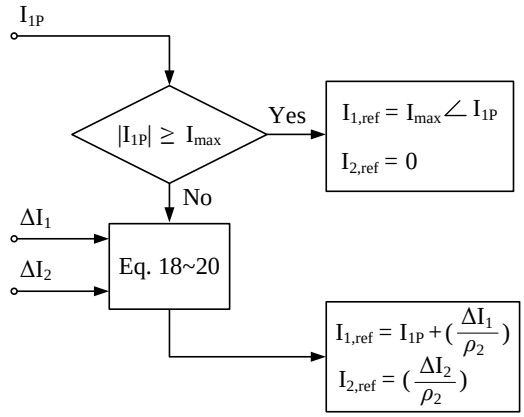

Figure 6. Proposed reference currents generator for active current priority mode

IV. Simulation Study

The simulation studies have been conducted on the test system shown in Fig. 7. The IBR is modeled in details in the PSCAD/EMTDC program. The IBR type is a full-converter interfaced photovoltaic power plant with the rated capacity of 50-MVA, connected to the grid through an YNd11, 16/230-kV, 50-MVA generator step-up (GSU) transformer. The maximum allowable current of the IBR is 1.2 pu, and k_1 and k_2 factors of the dynamic currents characteristics are both set to 5. As shown, the relay under study is installed at substation B and protects the line AB. Further details of the simulated system are presented in Appendix.

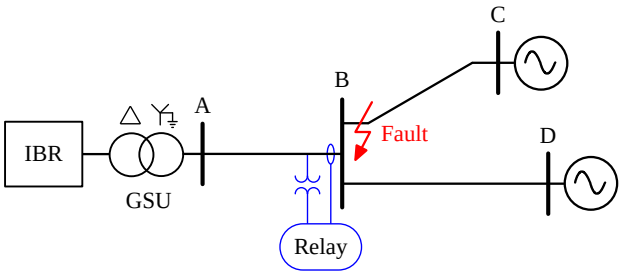

Figure 7. Single-line diagram of the simulated system

A number of simulations are performed for various fault types including 1-ph-g, ph-ph, 2-ph-g and 3-ph with a variable fault resistance from 0 to 50 Ohm at different points of the transmission system. However, due to limited space, just some illustrative cases in which the prevalent protective relays are prone to malfunction are presented here.

A. Single-Phase-to-Ground (1-ph-g) Fault on Line BC

This section presets the obtained results for an external AG fault with a fault resistance of 1 Ohm at 1 km distance from bus B on the line BC.

1) Reactive Current Priority Mode: Fig. 8 depicts the voltages and currents measured at the IBR POC, i.e. the low voltage side of the GSU transformer. Prior to the fault, the IBR is generating the rated power at the unity power factor. By the fault occurrence, the current in phase-B is reduced to about zero, while the magnitude of currents in phase-A and phase-C is increased to about 1.2 pu. It is worth noting that a 1-ph-g fault at the YN side of the transformer is seen as a phase-to-phase fault at its d side.

In this case, ΔV_1 and ΔV_2 at the POC are respectively equal to -0.24 and +0.24 pu. Since k_1 and k_2 are both set to 5, the dynamic positive- and negative-sequence currents' references will be equal to -1.2 and 1.2 pu. Here, the moderator factor calculated in (8) is 1.76. It means that the calculated references must be reduced to limit the inverter currents to 1.2 pu, while the full capacity of the inverter must be assigned for injecting dynamic reactive currents. Accordingly, the reference currents of the IBR calculated from (9) and (10) will be -0.68 and +0.68 pu.

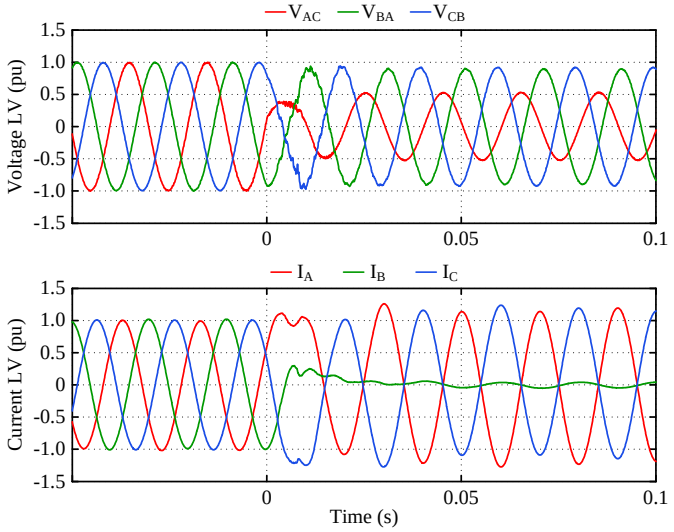

Figure 8. Voltages and currents at the POC for the AG fault case under reactive current priority mode

Fig. 9 depicts the voltages and currents measured at the relaying location shown in Fig. 7. As can be seen, since the short-circuit fault is very close to bus B, the voltage of faulty phase drops to almost zero. Although the inverter currents are limited to 1.2 pu, the magnitude of the current in phase-A at the relaying location is about 3.62 pu. This is because in effectively grounded transmission systems, the grounded neutral point of the GSU transformer provides a source of zero-sequence current during ground faults. Fig. 10(a) shows the response of the conventional cross-polarized directional algorithm. For phase-A that has picked up, the operating and reference quantities are I_A and V_{BC}, respectively. As can be seen, the fault is correctly identified in the reverse direction. Fig. 10(b) shows the impedance trajectory measured by AG measuring unit of the conventional distance relay. As can be seen, the measured impedance converges to a point behind the relay, correctly.

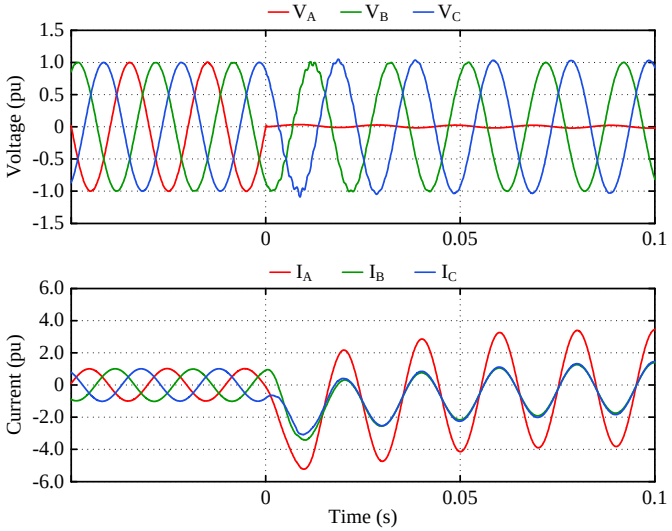

Figure 9. Voltages and currents at the relay location for the AG fault case under reactive current priority mode

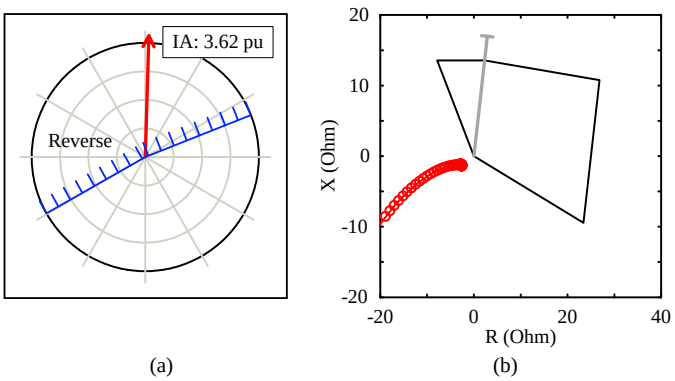

Figure 10. Response of conventional relays corresponding to Fig. 9, (a) cross-polarized directional algorithm, (b) AG measuring unit of distance relay

2) Active Current Priority Mode: Fig. 11 depicts the voltages and currents measured at the IBR POC. Prior to the fault, the IBR is generating the rated power at the unity power factor. By the fault occurrence, the positive-sequence voltage drops to 0.64 pu. Therefore, to inject the available active power into the grid, the positive-sequence active current calculated in (17) increases to 1.55 pu, which is greater than the maximum allowable current of the inverter. Thus, the reference of positive-sequence active current is limited to 1.2 pu, while no capacity will be available for injection of dynamic reactive currents.

Fig. 12 depicts the voltages and currents measured at the relaying location. Although the inverter currents are limited to 1.2 pu, the magnitude of the current in phase-A and phase-B at the relaying location are about 2.24 and 3.2 pu, respectively. This is because of the additional zero-sequence current that flows though the neutral point of the GSU transformer toward the fault point. As can be seen, although the fault does not involve phase-B, the magnitude of current in phase-B is even greater than that of the faulted phase-A.

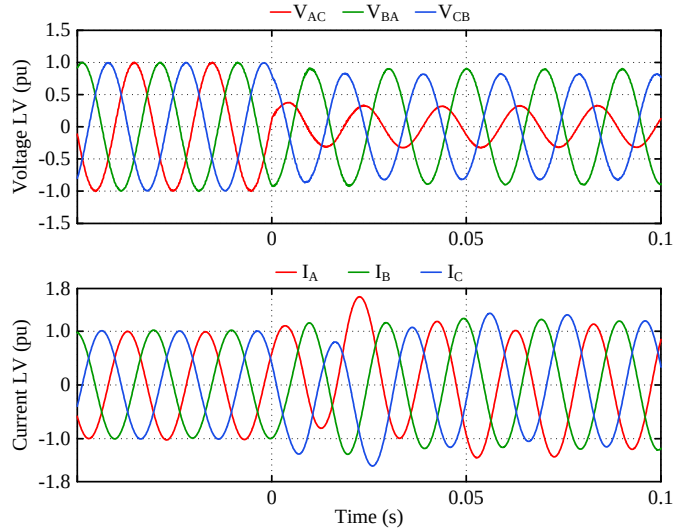

Figure 11. Voltages and currents at the POC for the AG fault case under active current priority mode

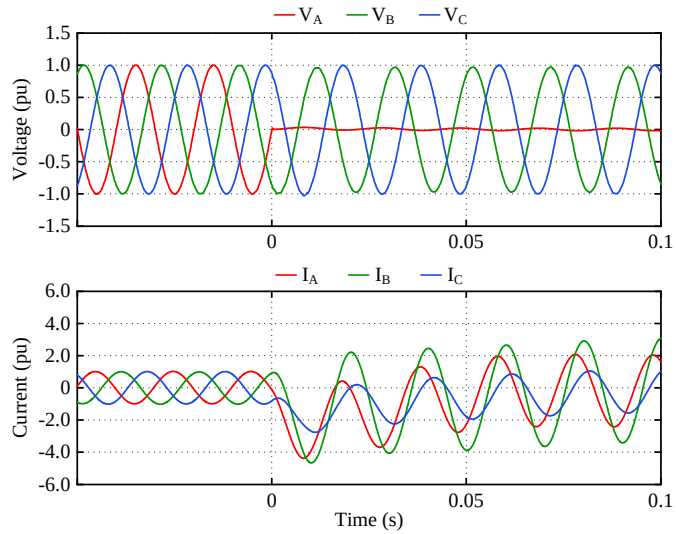

Figure 12. Voltages and currents at the relay location for the AG fault case under active current priority mode

Fig. 13 shows the response of the conventional protective algorithms. It can be observed that the element B of the cross polarized directional algorithm identifies the fault in the forward direction, incorrectly. Therefore, if the fault type classification algorithm is only based on the magnitude of phases currents, such a condition could lead to an incorrect decision. Figs. 13(c) and (d) show the impedance trajectory measured by the AG and BG measuring units of the distance relay. As can be seen, the impedance measured by unit AG converges to a point behind the relay, correctly. Meanwhile, the impedance measured by unit BG does not enter the relay operating zone.

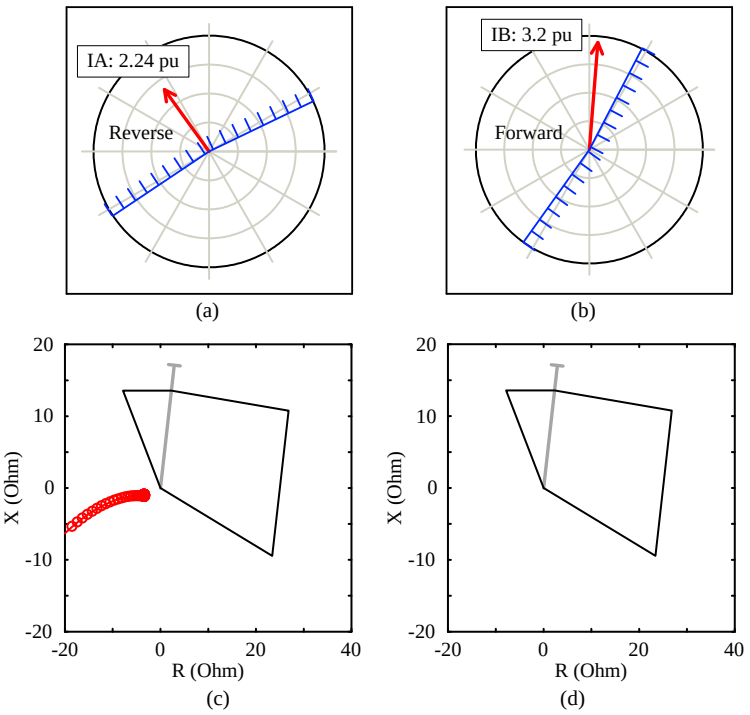

Figure 13. Response of conventional relays corresponding to Fig. 12, (a)-(b) cross- polarized directional algorithm, (c)-(d) AG and BG measuring unit of distance relay

B. *Phase-to-Phase (ph-ph) Fault on Line BC*

This section presets the obtained results for an external AB fault with a fault resistance of 1 Ohm at 1 km distance from bus B on the line BC.

1) Reactive Current Priority Mode: Fig. 14 depicts the voltages and currents measured at the IBR POC. In this case, ΔV_1 and ΔV_2 at the POC are respectively equal to -0.42 and +0.42 pu. Since k_1 and k_2 are both set to 5, the dynamic positive- and negative-sequence currents' references will be equal to -2.1 and 2.1 pu. Here, the moderator factor calculated in (8) is 3.5. It means that the calculated references must be reduced to limit the inverter currents to 1.2 pu, while the full capacity of the inverter must be assigned for injecting dynamic reactive currents. Accordingly, the reference currents of the IBR calculated from (9) and (10) will be -0.6 and +0.6 pu.

Fig. 15 depicts the voltages and currents measured at the relaying location. Prior to the fault, the IBR is generating the rated power at the unity power factor. It can be observed that although the magnitude of short-circuit current at the inverter output is capped by 1.2 pu, the currents magnitudes of the faulted phases at the grid side are about 1.04 pu. Meanwhile, the current in phase-C is almost zero.

Fig. 16 shows the response of the conventional protective relays. As can be seen, the fault is correctly identified in the reverse direction by elements A and B of the cross polarized directional algorithm. Meanwhile, the impedance measured by AB unit of the distance relay converges to a point behind the relay, correctly.

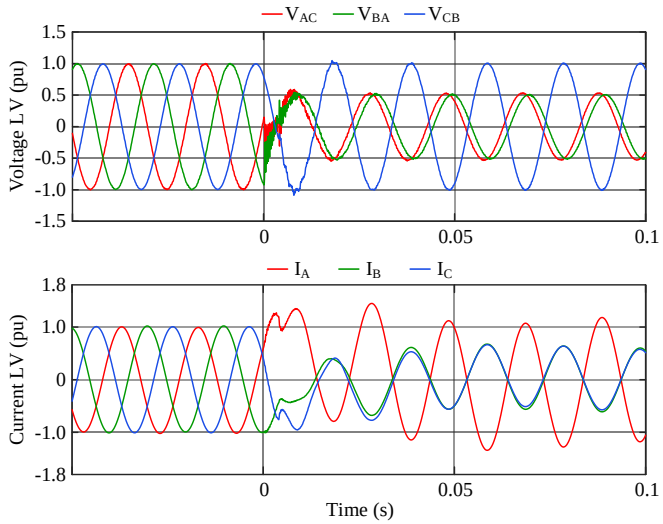

Figure 14. Voltages and currents at the POC for the AB fault case under reactive current priority mode

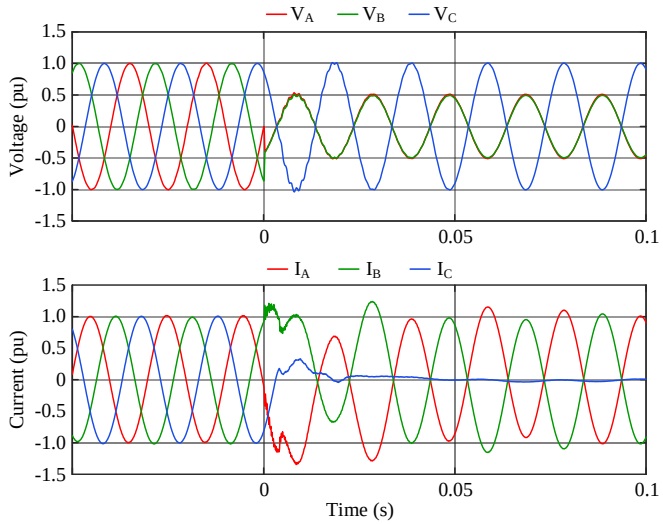

Figure 15. Voltages and currents at the relay location for the AB fault case under reactive current priority mode

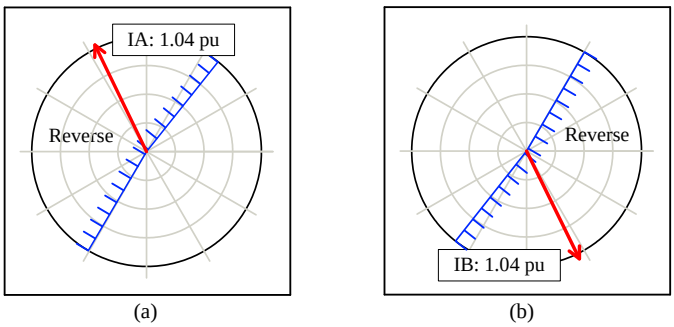

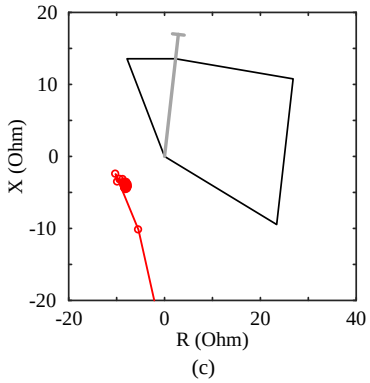

Figure 16. Response of conventional relays corresponding to Fig. 15, (a)-(b) cross- polarized directional algorithm, (c) AB measuring unit of distance relay

2) Active Current Priority Mode: Fig. 17 depicts the voltages and currents measured at the IBR POC. Prior to the fault, the IBR is generating the rated power at the unity power factor. By the fault occurrence, the positive-sequence voltage drops to 0.47 pu. Therefore, to inject the available active power into the grid, the positive-sequence active current calculated in (17) increases to 2.1 pu, which is greater than the maximum allowable current of the inverter. Thus, the reference of positive-sequence active current is limited to 1.2 pu, while no capacity will be available for injection of dynamic reactive currents.

Fig. 18 depicts the voltages and currents measured at the relaying location. As can be seen, although the fault does not involve phase-C, the current magnitude in all phases is equal to 1.2 pu. Fig. 19 shows the response of the conventional protective algorithms. It can be observed that the elements B and C of the cross polarized directional algorithm identify the fault in the forward direction, incorrectly. Furthermore, the impedance measured by the BG measuring unit of the distance relay enters the relay forward zone, incorrectly.

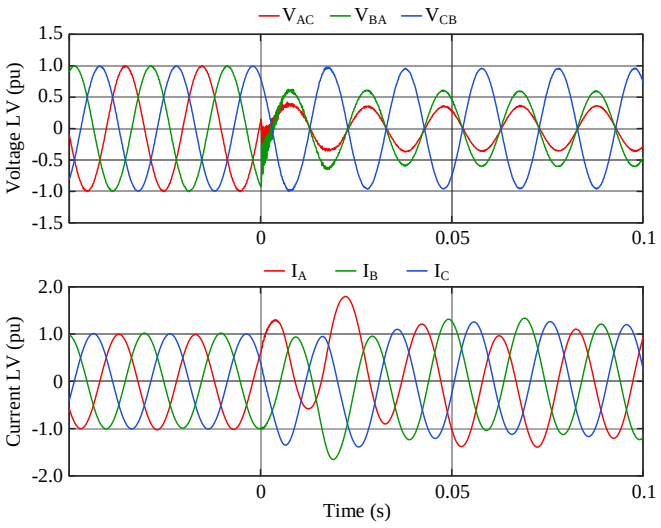

Figure 17. Voltages and currents at the POC for the AB fault case under active current priority mode

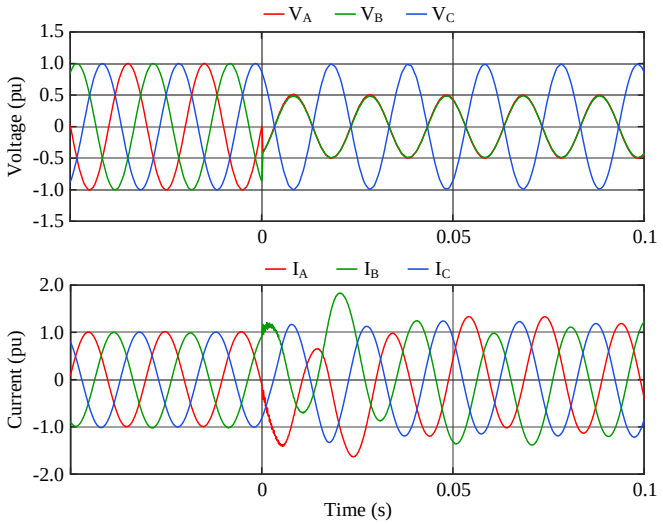

Figure 18. Voltages and currents at the relay location for the AB fault case under active current priority mode

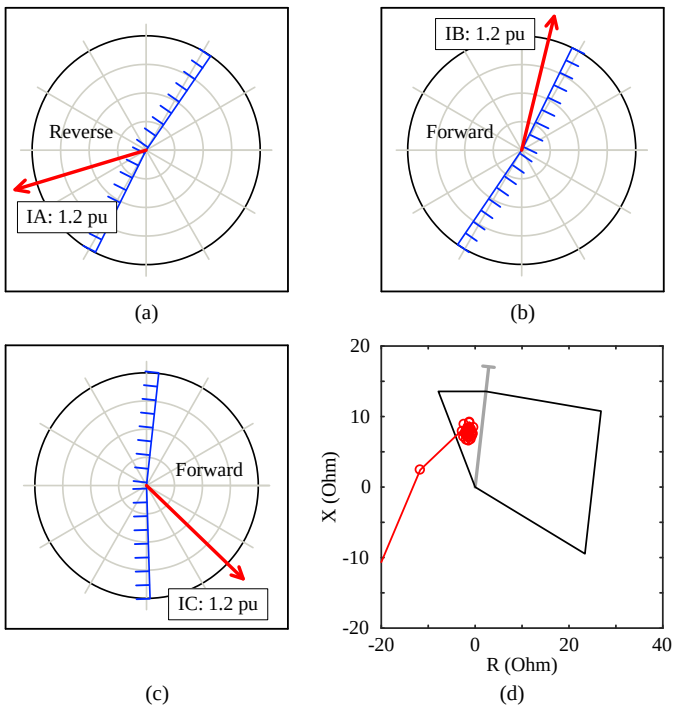

Figure 19. Response of conventional relays corresponding to Fig. 18, (a)-(c) cross- polarized directional algorithm, (d) AB measuring unit of distance relay

V. Conclusion

This paper presented a comprehensive study on the comparison of current control modes specified in IEEE Std. 2800-2022 from the point of view of grid protective relays. For this purpose, a novel reference currents generator was proposed to comply with the requirements of the mentioned standard. Then, an IBR including its complete closed-loop control system was modeled in the PSCAD/EMTDC program, and extensive simulation studies were performed for various fault

types with different fault resistances at different points of a test transmission system. The obtained results indicate that the reactive current priority mode provides superior performance for the correct operation of grid protective relays. Whereas, the active current priority mode may lead to malfunction of conventional protective relays. It was observed that when the IBR is operating in active current priority mode, the conventional cross polarized directional algorithm may incorrectly identify a reverse fault in the forward direction. Meanwhile, a reverse fault may be seen inside the forward zone of the conventional distance relay.

REFERENCES

[1] Protection challenges and practices for interconnecting inverter based resources to utility transmission systems, IEEE Power & Energy Soc., pp. 1-65, July 2020.

[2] M. Patel, "Opportunities for standardizing response, modeling and analysis of inverter-based resources for short circuit studies," IEEE Transactions on Power Delivery, 36(4), pp. 2408-2415, 2020.

[3] B. Kasztenny, "Distance elements for line protection applications near unconventional sources," Schweitzer Engineering Laboratories, revised edition released, Jun. 2021.

[4] Z. Yang, W. Liao, Q. Zhang, C. L. Bak, and Z. Chen, "Fault coordination control for converter-interfaced sources compatible with distance protection during asymmetrical faults," IEEE Transactions on Industrial Electronics, vol. 70, no. 7, pp. 6941-6952, Sep. 2022.

[5] R. Chowdhury, and N. Fischer, "Transmission line protection for systems with inverter-based resources- Part I: Problems," IEEE Transactions on Power Delivery, 36(4), pp. 2416-2425, 2021.

[6] P. Jafarian, S. M. Hashemi, and M. Sanaye-Pasand, "Design of current reference controller for inverter-based resources to emulate short-circuit behavior of a synchronous generator," In 2023 International Conference on Protection and Automation of Power Systems (IPAPS), Tehran, Iran, pp. 1-7, Jan. 2023.

[7] Z. Yang, Z. Liu, Q. Zhang, Z. Chen, J. de Jesus Chavez, and M. Popov, "A control method for converter-interfaced sources to improve operation of directional protection elements," IEEE Trans. Power Del., vol. 38, no. 1, pp.642-654 , Feb. 2023.

[8] A. A. Aboelnaga, M. A. Azzouz, M.A., H. F. Sindi, and A. S. Awad, "Fault ride through of inverter-interfaced renewable energy sources for enhanced resiliency and grid code compliance," IEEE Transactions on Sustainable Energy, vol. 13, no. 4, pp.2275-2290, Oct. 2020.

[9] M. Zadeh, P. K. Mansani, and I. Voloh, "Impact of inverter-based resources on impedance-based protection functions," 46th Annual Western Protective Relay Conference, pp. 1-10. Oct. 2020.

[10] A. Banaiemoqadam, A. Hooshyar, and M. A. Azzouz, "A comprehensive dual current control scheme for inverter-based resources to enable correct operation of protective relays," IEEE Transactions on Power Delivery, 36(5), pp.2715-2729, 2020.

[11] A. Haddadi, M. Zhao, I. Kocar, U. Karaagac, K. W. Chan, and E. Farantatos,"Impact of inverter-based resources on negative-sequence quantities-based protection elements," IEEE Trans. Power Del., 36(1), pp.289-298, 2020.

[12] M. Nagpal and C. Henville, "Impact of power-electronic sources on transmission line ground fault protection," IEEE Trans. Power Del., vol. 33, no. 1, pp. 62–70, Feb. 2018.

[13] VDE-AR-N 4130, Technical Requirements for the Connection and Operation of Customer Installations to the Extra High Voltage Network (TCR Extra High Voltage), Nov. 2018.

[14] IEEE Standard for Interconnection and Interoperability of Inverter-Based Resources (IBRs) Interconnecting with Associated Transmission Electric Power Systems, IEEE Power and Energy Society, IEEE Std. 2800, 2022.

APPENDIX

The details of the simulated system are given in Table I.

TABLE I. INFORMATION OF THE SIMULATED SYSTEM

Transmission-lines	V_n = 230 kV
	Z_1 = 0.072 + j0.424 Ohm/km
	Z_0 = 0.327 + 1.17 Ohm/km
	Line AB: Length = 40 km
	Line BC: Length = 46 km
	Line BD: Length = 90 km
Source C	Z_1 = 3.84 + j 109.93 Ohm
	Z_0 = 4.54 + j 129.92 Ohm
Source D	Z_1 = 2.79 + j 79.95 Ohm
	Z_0 = 3.14 + j 89.94Ohm